[CANCER RESEARCH 59, 5209–5218, October 15, 1999]

# Antivascular Endothelial Growth Factor Receptor (Fetal Liver Kinase 1) Monoclonal Antibody Inhibits Tumor Angiogenesis and Growth of Several Mouse and Human Tumors

**Marie Prewett, James Huber, Yiwen Li, Angel Santiago, William O'Connor, Karen King, Jay Overholser, Andrea Hooper, Bronislaw Pytowski, Larry Witte, Peter Bohlen, and Daniel J. Hicklin[1]**

*Departments of Immunology [M. P., J. H., Y. L., W. O., K. K., J. O., A. H., D. J. H.], Molecular and Cell Biology [A. S., B. P., L. W.], and Research [P. B.], ImClone Systems Inc., New York, New York 10014*

## ABSTRACT

**Tumor angiogenesis is mediated by tumor-secreted angiogenic growth factors that interact with their surface receptors expressed on endothelial cells. Vascular endothelial growth factor (VEGF) and its receptor [fetal liver kinase 1 (Flk-1)/kinase insert domain-containing receptor] play an important role in vascular permeability and tumor angiogenesis. Previously, we reported on the development of anti-Flk-1 and antikinase insert domain-containing receptor monoclonal antibodies (mAbs) that potently inhibit VEGF binding and receptor signaling. Here, we report the effect of anti-Flk-1 mAb (DC101) on angiogenesis and tumor growth. Angiogenesis *in vivo* was examined using a growth factor supplemented (basic fibroblast growth factor + VEGF) Matrigel plug and an alginate-encapsulated tumor cell (Lewis lung) assay in C57BL/6 mice. Systemic administration of DC101 every 3 days markedly reduced neovascularization of Matrigel plugs and tumor-containing alginate beads in a dose-dependent fashion. Histological analysis of Matrigel plugs showed reduced numbers of endothelial cells and vessel structures. Several mouse tumors and human tumor xenografts in athymic mice were used to examine the effect of anti-Flk-1 mAb treatment on tumor angiogenesis and growth. Anti-Flk-1 mAb treatment significantly suppressed the growth of primary murine Lewis lung, 4T1 mammary, and B16 melanoma tumors and growth of Lewis lung metastases. DC101 also completely inhibited the growth of established epidermoid, glioblastoma, pancreatic, and renal human tumor xenografts. Histological examination of anti-Flk-1 mAb-treated tumors showed evidence of decreased microvessel density, tumor cell apoptosis, decreased tumor cell proliferation, and extensive tumor necrosis. These findings support the conclusion that anti-Flk-1 mAb treatment inhibits tumor growth by suppression of tumor-induced neovascularization and demonstrate the potential for therapeutic application of anti-VEGF receptor antibody in the treatment of angiogenesis-dependent tumors.**

## INTRODUCTION

Angiogenesis, the formation of new blood vessels from existing vasculature, is a tightly regulated event playing an important role in embryonic development, follicular growth, wound healing, and pathological conditions such as tumor growth and progression (1, 2). Growth and metastasis of primary solid tumors is dependent on formation of new blood vessels. In the absence of neovascularization, tumors become necrotic or apoptotic and/or fail to grow beyond 2–3 $mm^3$ in size (3). Tumor angiogenesis involves several processes, including endothelial cell activation, proliferation, migration, and tissue infiltration from preexisting blood vessels that are triggered by specific angiogenic growth factors produced by tumor cells and the surrounding stroma (1–4). Several growth factors have been identified as possible regulators of angiogenesis (5). Among these factors, VEGF[2] (2) and its receptors are thought to play a key role in tumor angiogenesis (6–9).

VEGF is a homodimeric 34–42 kDa heparin-binding glycoprotein with potent angiogenic, mitogenic, and vascular permeability-enhancing activities (10, 11). VEGF regulates vasculogenesis during embryonic development and angiogenic processes during adult life (12, 13). VEGF binds to and mediates its activity through the Flt-1 (14) and Flk-1 (KDR in humans; Refs. 15 and 16) kinase receptors. The physiological importance of VEGF and the VEGF receptors in blood vessel formation has been clearly demonstrated in gene knockout experiments. Targeted deletion of genes encoding VEGF (17), Flt-1 (14), or Flk-1 (18) in mice is embryonic lethal. VEGF, Flt-1, and Flk-1 null mice fail to develop normal vasculature that is manifested by impaired blood island formation and vasculogenesis and a defect in endothelial cell development. These studies also suggest that Flt-1 receptor regulates endothelial cell-cell or cell matrix interactions, whereas the Flk-1 receptor is important for endothelial cell differentiation and mitogenesis.

Numerous studies have shown that overexpression of VEGF and Flk-1/KDR is strongly associated with invasion and metastasis in human malignant disease (for review, see Ref. 6). VEGF is expressed at high levels in various types of tumors (12, 19), and newly sprouting capillaries are clustered around VEGF-producing tumor cells (12). VEGF expression is strongly up-regulated under hypoxic conditions, such as those associated with rapidly growing tumors (20). VEGF and VEGF receptors have been implicated in angiogenesis that occurs in many human solid tumors, including bladder (21), breast (22, 23), colon (24, 25), gastrointestinal (26), glioma (12, 27), renal (28), melanoma (29), and neuroblastoma (30). The important role for VEGF and Flk-1/KDR in tumor angiogenesis was directly demonstrated in studies in which expression of a dominant-negative Flk-1 receptor resulted in decreased endothelial cell mitogenesis and growth inhibition of s.c. glioma tumors in athymic mice (31). Other studies using antisense against VEGF (32), neutralization of VEGF by mAbs (33), neutralizing soluble VEGF receptor (34, 35), or Flk-1/KDR kinase inhibitors (36) were also shown to inhibit angiogenesis and tumor growth.

The importance of the Flk-1/KDR receptor in tumor angiogenesis suggests that blockade of this receptor would be a useful therapeutic strategy for inhibiting angiogenesis and tumor growth. Previously, we described the development of anti-Flk-1 (37) and anti-KDR (38, 39) mAb generated against the extracellular domain of each receptor. These mAb are potent antagonists for VEGF binding, Flk-1/KDR receptor signaling, and VEGF-induced endothelial cell growth *in vitro*. In this report, we analyzed the effect of VEGF receptor block-

Received 6/3/99; accepted 8/20/99.

The costs of publication of this article were defrayed in part by the payment of page charges. This article must therefore be hereby marked *advertisement* in accordance with 18 U.S.C. Section 1734 solely to indicate this fact.

[1] To whom requests for reprints should be addressed, at Department of Immunology, ImClone Systems Inc., 180 Varick St., New York, NY 10014. Phone: (212) 645-1405; Fax: (212) 645-2054; E-mail: danh@imclone.com.

[2] The abbreviations used are: VEGF, vascular endothelial growth factor; Flt-1, fms-like tyrosine kinase 1; Flk-1, fetal liver kinase 1; KDR, kinase insert domain-containing receptor; mAb, monoclonal antibody; bFGF, basic fibroblast growth factor; TUNEL, terminal deoxynucleotidyltransferase-mediated dUTP nick end labeling; DAB, diaminobenzidine tetrachloride; PECAM, platelet/endothelial cell adhesion molecule; RT, room temperature; HRP, horseradish peroxidase; PCNA, proliferating cell nuclear antigen.

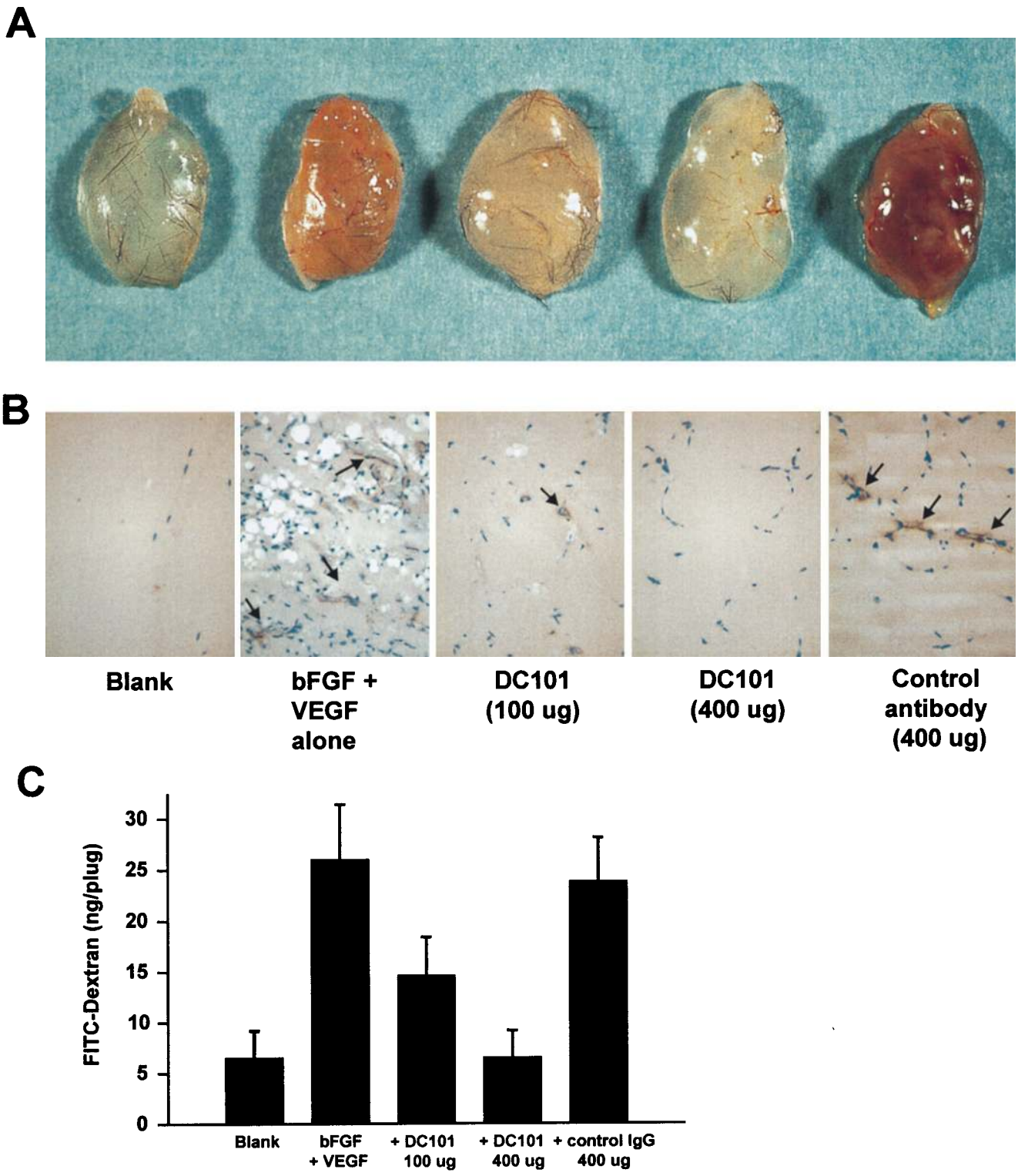


Fig. 1. Anti-Flk-1 mAb inhibits vascularization of Matrigel plugs. C57BL/6 mice were injected s.c. at the abdominal midline with 0.5 ml of Matrigel with or without bFGF and $VEGF_{165}$. Anti-Flk-1 mAb DC101 or control rat antibody was administered i.p. every 3 days starting 24 h after Matrigel injection. Matrigel plugs were removed 21 days after implantation, photographed, and prepared for histological examination or FITC-dextran uptake. *A,* photomicrograph of Matrigel plugs removed from mice after 21 days showing reduction in plug vascularization by anti-Flk-1 mAb treatment. *B,* immunohistochemical staining of sections of Matrigel plugs with anti-PECAM antibody shows reduced numbers of endothelial cells and vessel structures (*arrows*) in DC101-treated plugs. ×200. *C,* Matrigel plug vascularization was quantitated by FITC-dextran uptake into plugs as described in "Materials and Methods." DC101 significantly ($P < 0.01$ at 400 $\mu$g compared to control) reduced plug vascularization as measured by FITC-dextran uptake. *Columns,* mean of 12 mice/group; *bars,* SE.

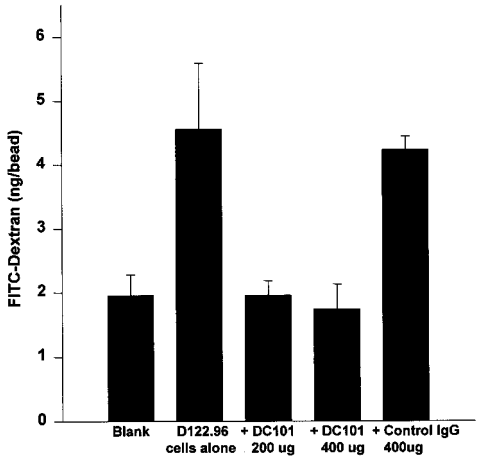


Fig. 2. Anti-Flk-1 mAb inhibits tumor cell-induced angiogenesis. Alginate beads containing $5 \times 10^4$ D122-96 cells were implanted s.c. into C57BL/6 mice. DC101 was administered i.p. every 3 days beginning 1 day after bead implantation. Beads were surgically removed and FITC-dextran quantified as outlined in "Materials and Methods." *Columns,* mean of 12 mice/group; *bars,* SE.

ade by anti-Flk-1 mAb in *in vivo* models of angiogenesis and on tumor growth in several mouse and human xenograft tumor models.

## MATERIALS AND METHODS

**Cell Lines.** The 4T1 mouse mammary carcinoma cell line was provided by Dr. H. K. Lyerly (Duke University, Durham, NC). The B16.F10 mouse melanoma cell line was provided by Dr. I. J. Fidler (M. D. Anderson Cancer Center, Houston, TX). The mouse Lewis lung carcinoma (clone D122-96) was obtained from Dr. L. Eisenbach (Weizman Institute of Science, Rehovot, Israel). The human glioblastoma cell line (GBM-18) was provided by Dr. P. Fisher (Columbia University, New York, NY). Human renal cell carcinoma cell line SK-RC-29 was provided by Dr. N. Bander (New York Hospital-Cornell University Medical Center, New York, NY). The A431 human epidermoid carcinoma and the BxPC-3 pancreatic carcinoma cell lines were obtained from the American Type Culture Collection (Manassas, VA). All cell lines were maintained in DMEM (Life Technologies, Inc., Gaithersburg, MD) containing 10% FBS (HyClone Laboratories, Logan, UT).

**Animals.** Five- to 6-week-old female C57BL/6, BALB/c and athymic nu/nu mice were purchased from Harlan Sprague Dawley, Inc. (Indianapolis, IN). Mice were housed under pathogen-free conditions in microisolator cages with laboratory chow and water available *ad libitum*. Animals were anesthetized before all procedures and observed until fully recovered. All experiments and procedures were reviewed by the ImClone Institutional Review Committee and performed in accordance with the United States Department of Agriculture, Department of Health and Human Services, and NIH polices regarding the humane care and use of laboratory animals.

**Anti-Flk-1 Antibody.** The rat anti-Flk-1 mAb DC101 was developed and characterized as described previously (37). Hybridoma cells were grown via continuous feed fermentation in serum-free medium. mAb DC101 was purified from conditioned media by a multistep chromatography process and assessed for purity in SDS-PAGE and immunoreactivity with soluble Flk-1 receptor (40) by ELISA. The negative control polyclonal rat IgG was purchased from Jackson ImmunoResearch Laboratories (West Grove, PA). DC101 and control rat IgG were tested for endotoxin using the Pyrogent Plus *Limulus* amebocyte lysate kit (BioWhittaker, Walkersville, MD). All antibody preparations used in animal studies contained $\leq$1.25 endotoxin units/ml of endotoxin.

**Matrigel Plug Assay.** Matrigel plug assays were performed as described previously with modifications (41). C57BL/6 mice were anesthetized and injected s.c. at the abdominal midline with 0.5 ml of Matrigel (Becton Dickinson, Bedford, MA) supplemented with 500 ng of bFGF (R&D Systems, Minneapolis, MN) and 10 $\mu$g of $VEGF_{165}$ (40). Control mice were injected with Matrigel without added growth factors. Anti-Flk-1 mAb or control rat antibody were administered i.p. every 3 days starting 24 h after Matrigel injection. Matrigel plugs were removed 21 days postimplantation, photographed, and prepared for histological examination. Vascularization of plugs was quantitated by injecting mice on day 21 i.v. with 0.1 ml of a 100 mg/kg FITC-dextran solution (molecular weight, ~150,000; Sigma Chemical Co., St. Louis, MO). After 20 min, mice were sacrificed, and Matrigel plugs were removed and transferred to tubes containing 0.5 ml of Dispase reagent (Becton Dickinson). Plugs were incubated for 1 h at 37°C and then ground with a hand-held mixer. Sterile saline was added to the tubes, which were then vortexed and centrifuged at 2000 rpm for 5 min. Fluorescence of the supernatant was measured in a fluorometer (Turner model 450; excitation at 492 nm, measurement at 515 nm) and quantitated against a standard curve of FITC-dextran.

**Alginate Encapsulation Assay.** Alginate encapsulated tumor cell assays were performed as described previously with modifications (42). Briefly, D122-96 tumor cells were resuspended in a 1.5% solution of sodium alginate and added dropwise into a swirling 37°C solution of 250 mM calcium chloride. Alginate beads were formed containing approximately $5 \times 10^4$ tumor cells per bead. C57BL/6 mice were then anesthetized, and four beads were implanted s.c. into an incision made on the dorsal side. Incisions were closed with surgical clamps. DC101 or control IgG treatment was started 24 h after bead implantation and injected i.p. every 3 days. After 12 days, mice were injected i.v. with 100 $\mu$l of a 100 mg/kg FITC-dextran solution. Animals were sacrificed, and beads removed and incubated overnight at RT in 1 ml of Tris buffer (1 mM Tris-HCl, pH 8). The beads were ground briefly with a hand-held mixer, and an additional 1 ml of Tris buffer was added. Samples were then vortexed and centrifuged at 1500 rpm for 5 min. Fluorescence of the sample supernatants was quantitated against a standard curve of FITC-dextran.

**Mouse Tumor Models.** s.c. murine Lewis lung ($2 \times 10^6$ cells), B16 melanoma or 4T1 breast tumors ($10^5$ cells) were established by injecting C57BL/6 or BALB/c mice, respectively, s.c. in the right flank. Three days later, mice received an i.p. injection of various doses of DC101 or rat IgG every 3 days. Tumors were measured twice weekly with calipers, and tumor volumes were calculated by the formula $[\pi/6\ (w_1 \times w_2 \times w_2)]$, where $w_1$ represents the largest tumor diameter and $w_2$ represents the smallest tumor diameter. For the pulmonary metastasis model, mice were injected intrafootpad with $1 \times 10^5$ D122-96 tumor cells (43). When footpad tumors reached 5 mm in diameter, the tumor-bearing leg was surgically ligated. Mice were then divided into two groups receiving i.p. injections of 27 mg/kg/dose of either DC101 or control IgG every 3 days for 3 weeks. Mice were sacrificed, and the lungs removed and weighed to measure the metastatic load. Tumor nodules on the lung surface were also counted as described previously (43).

**Human Tumor Xenograft Models.** s.c. human epidermoid (A431), renal cell carcinoma (SK-RC-29), pancreatic (BxPC-3) or glioblastoma (GBM-18) tumors were established by injecting athymic nude mice s.c in the right flank with $2 \times 10^6$ tumor cells mixed in Matrigel. Tumors were allowed to reach 150–200 $mm^3$ in size, and then randomized groups of 10 animals received i.p. injections of DC101 or control IgG (27 mg/kg/dose) every 3 days. Tumors were measured twice weekly with calipers, and tumor volumes were calculated as described above. Tumor permeability in DC101-treated and control animals was analyzed by injecting mice bearing human tumor xenografts i.v. with 300 $\mu$l of a 1% solution of Evans blue (44). After 45 min, mice were perfused with saline, and tumors were removed and photographed.

**Histology.** Matrigel plugs were resected, fixed in 10% neutral buffered formalin for 4 h at 4°C, paraffin embedded, and sectioned at 10 $\mu$m. Sections of Matrigel plugs were digested with 0.1% papain for 15 min at RT followed by an incubation with 3% $H_2O_2$ for 10 min at RT. Mouse vessels were stained with a rabbit anti-von Willebrand factor antibody (DAKO Corp., Carpinteria, CA) at a final concentration of 20 $\mu$g/ml. Sections were then incubated with biotin-labeled goat antirabbit IgG (Biosource, Camarillo, CA) for 30 min at RT followed by incubation with streptavidin-HRP (Jackson ImmunoResearch) for 20 min at RT. Sections were developed with 3,3′-DAB (Zymed, San Francisco, CA). Isotype control staining was carried out for all specimens. Sections were counterstained with hematoxylin.

Tumor tissue was fixed in 10% neutral buffered formalin overnight at 4°C, paraffin embedded, and sectioned for examination of vessel density, tumor cell proliferation, and apoptosis. Staining of tumor tissue for mouse vessels was performed by incubating sections with a rat antimouse PECAM mAb (MEC13.3, 1 $\mu$g/ml, PharMingen) for 30 min at 37°C. Sections were then incubated with a biotin-labeled goat antirat IgG (Biosource) for 30 min at RT and were developed with DAB and counterstained with hematoxylin. PCNA

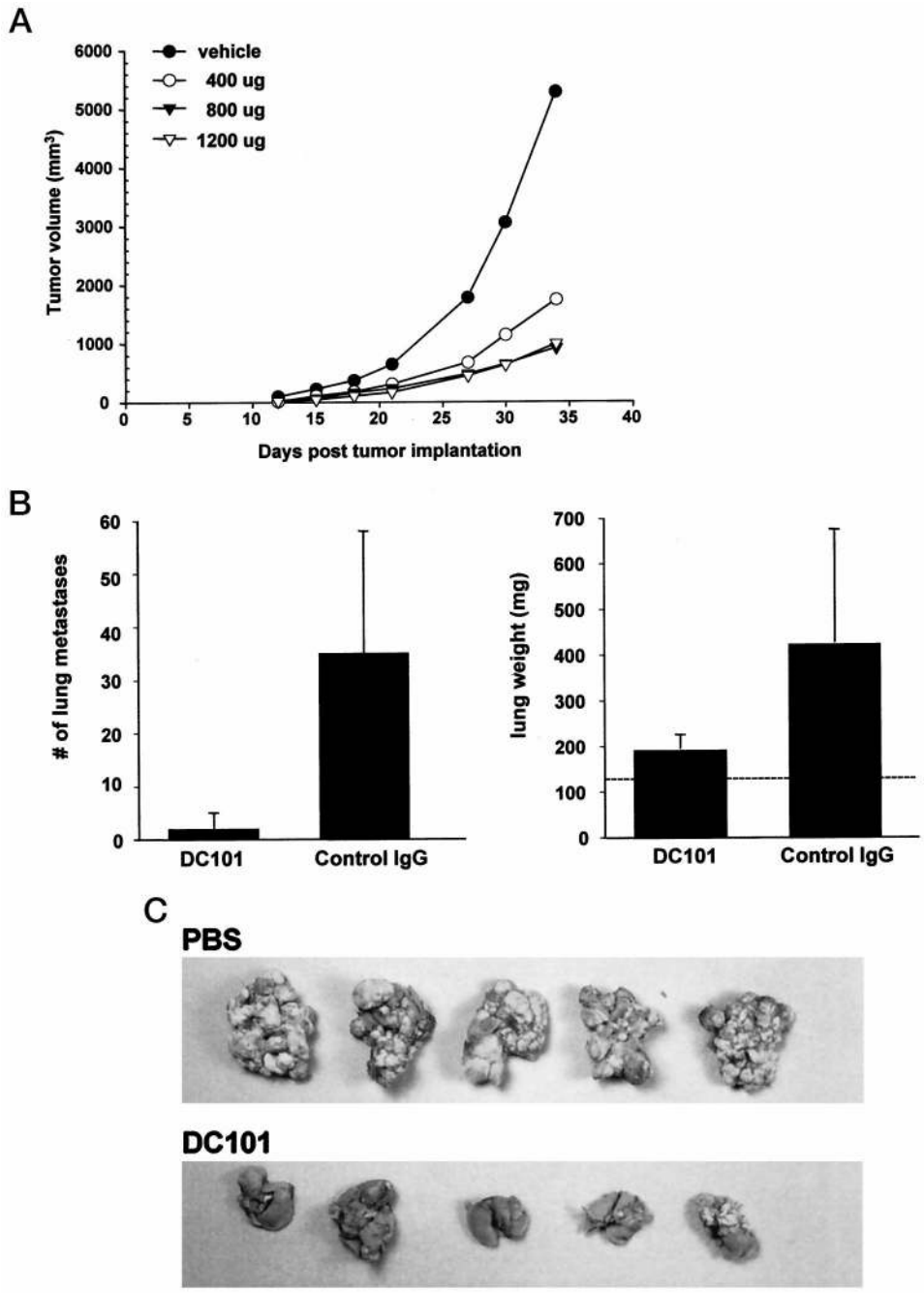


Fig. 3. Anti-Flk-1 treatment inhibits growth of s.c. Lewis lung tumors and metastases. *A,* s.c. Lewis lung tumors were established by injecting $1 \times 10^6$ D122 cells into the right flank of C57BL/6 mice. After 3 days, mice received i.p. injections of either DC101 or control IgG every 3 days. Tumor volumes were measured twice weekly as described in "Materials and Methods" and are shown as mean of 10 mice/group. *B,* mice were injected intra-footpad with $1 \times 10^5$ D122-96 tumor cells. When footpad tumors reached 5 mm in diameter, the tumor-bearing leg was surgically ligated. Mice were then divided into two groups receiving i.p. injections of either DC101 (800 $\mu$g/dose) or PBS every 3 days for 3 weeks. Mice were then sacrificed, the lungs were removed, tumor nodules were counted, and lungs were weighed to measure the metastatic load. *Columns,* mean of 10 mice/group; *bars,* SE. *Dashed line,* average weight of normal lung. *C,* photomicrograph of representative lungs from mice in control group (*top*) or the DC101 treatment group (*bottom*).

was detected using an antibody directly conjugated to HRP (EPOS system, DAKO Corp.). The sections were developed with DAB and counterstained with Light Green counterstain (Biomeda, Foster City, CA). TUNEL staining was performed using an *in situ* cell death detection kit (Boehringer Mannheim). Sections were digested for 15 min at RT with proteinase K (20 $\mu$g/ml), permeabilized with 0.1% sodium citrate buffer containing 0.1% Triton X-100 for 2 min at 4°C, and blocked for 1 h with 1× universal blocker (Biogenex, San Ramon, CA). Sections were incubated with the TUNEL labeling mix at 37°C for 1 h. Light and fluorescent images of immunostained tissue were viewed on a Zeiss Axioskop and digitized using a SONY camera and Scion CG-7 framegrabber. Vessel density was captured using NIH Image software and quantitated by analyzing 10 random fields per section (from three mice in each group) using Corel PhotoPaint.

**Statistical Analysis.** Tumor volume, lung metastases, and vessel density counts were analyzed using the Student's *t* test. Analyses were computed using the statistical package in SigmaStat version 2.0 (Jandel Scientific, San Rafael, CA).

## RESULTS

**Anti-Flk-1 mAb Inhibits Vascularization of Matrigel Plugs and Tumor-induced Angiogenesis of Alginate Implants.** To demonstrate that anti-Flk-1 mAb can directly inhibit angiogenesis *in vivo,* we tested DC101 in two models. In the first, Matrigel supplemented with bFGF and VEGF was injected s.c. into C57BL/6 mice, forming semi-solid plugs. Twenty-four h later, mice were treated with DC101 mAb or control rat IgG every 3 days for a total of 21 days. Plugs without growth factors had virtually no vascularization or vessel structures after 21 days (Fig. 1). In contrast, plugs supplemented with bFGF and VEGF had extensive vascularization and vessels throughout the plug. Plugs taken from mice treated with 100 or 400 $\mu$g of DC101 antibody had markedly reduced vascularization of plugs (Fig. 1*A*). Furthermore, histological examination of plugs showed decreased vessel staining (Fig. 1*B*). Matrigel plug angiogenesis was

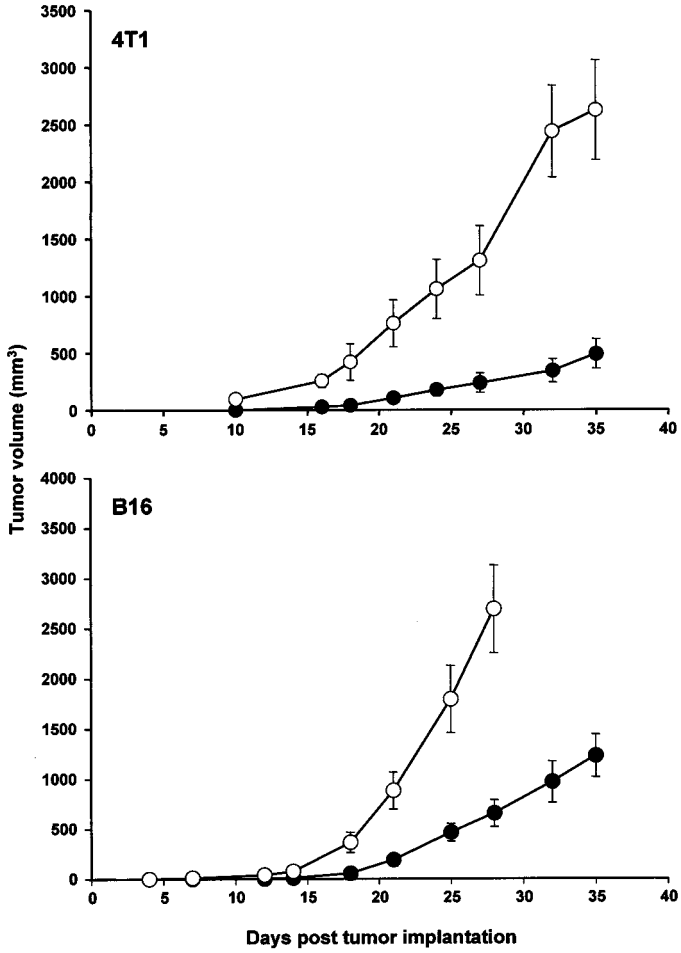


Fig. 4. Anti-Flk-1 treatment inhibits growth of s.c. 4T1 and B16 tumors. s.c. 4T1 and B16 tumors were established by injecting $1 \times 10^6$ tumor cells into the right flank of BALB/c and C57BL/6 mice, respectively. After 3 days, mice received i.p. injections of either DC101 (●; 800 $\mu$g/dose) or an equivalent dose of control IgG (○) every 3 days. Tumor volumes were measured twice weekly as described in "Materials and Methods"; *data points,* mean of 10 mice/group; *bars,* SE.

quantitated by measuring the uptake of FITC-dextran into plugs prior to their removal from mice. DC101 treatment at 400 $\mu$g/dose significantly (>73%, $P < 0.01$) inhibited the amount of FITC-dextran in Matrigel plugs compared to control antibody (Fig. 1*C*).

The effect of anti-Flk-1 mAb on angiogenesis *in vivo* was also examined in an alginate-encapsulated tumor cell assay. Alginate beads containing Lewis lung tumor cells were implanted s.c. into the back of C57BL/6 mice. Growth factors produced by the encapsulated tumor cells induce vascularization of the beads over 12 days, which can then be measured by uptake of FITC-dextran. DC101 administered every 3 days significantly reduced the vascularization of alginate beads compared to mice injected with control antibody (Fig. 2). FITC-dextran uptake was decreased 52% for animals receiving a 200 $\mu$g/dose of DC101 and 68% ($P < 0.02$ *versus* control) for animals receiving 400 $\mu$g/dose.

**Inhibition of Mouse Tumor Growth and Metastasis.** To examine the antitumor activity of anti-Flk-1 mAb we tested DC101 in the Lewis lung, 4T1, and B16 mouse tumor models. Each of these tumor models exhibits aggressive tumor growth kinetics. To determine the sensitivity of Lewis lung tumors to anti-Flk-1 mAb therapy, we first performed a dose-response experiment. Untreated Lewis lung tumors reached a size of >3000 mm$^3$ within 30 days. By day 34, mice became moribund in the control group, and the experiment was terminated. DC101 treatment of mice bearing s.c. Lewis lung tumors inhibited tumor growth in a dose-dependent manner compared to control antibody (Fig. 3*A*). The maximal effective dose in this tumor model was 800 $\mu$g of DC101 administered every 3 days ($P < 0.01$ *versus* control IgG). No signs of toxicity, such as weight loss or lethargy in response to DC101 treatment, were observed. Pathological examination of tissues from treated mice also appeared normal.

DC101 mAb treatment was also tested in a Lewis lung metastasis model. Primary Lewis lung footpad tumors were removed when tumors reached 5 mm in size. As shown in Fig. 3, *B* and *C,* DC101 treatment significantly inhibited the growth of pulmonary metastases. Lung weight (54%) and metastases (94%) was significantly reduced ($P < 0.01$ and $P < 0.01$, respectively) in DC101-treated mice compared to the control group. In fact, 50% of the mice in the DC101-treated group had no macroscopic evidence of pulmonary metastases, whereas all mice in the control group had large numbers of lung metastases.

To compare the effects of anti-Flk-1 mAb therapy on other mouse tumors, we also tested DC101 in a mouse mammary carcinoma (4T1) and mouse melanoma (B16) models. DC101 treatment significantly inhibited the growth of 4T1 ($P < 0.02$) and B16 ($P < 0.05$) tumors compared to control antibody (Fig. 4). Mortality or morbidity in control groups due to tumor burden was observed at 35 and 27 days for the 4T1 and B16 models, respectively, whereas all mice in the DC101-treated groups survived beyond these time points. Growth of 4T1 tumors was inhibited 83% (day 35) compared to control animals, and B16 tumors were inhibited 75% (day 27; Table 1).

**Anti-Flk-1 mAb Inhibits Growth of Human Tumor Xenografts.** To examine the effect of anti-Flk-1 therapy on human tumor growth, athymic nude mice bearing established (>150 mm$^3$) epidermoid, glioblastoma, pancreatic, or renal xenograft tumors were treated systemically with DC101 (800 $\mu$g/dose) or control antibody every 3 days. As shown in Fig. 5, DC101 significantly inhibited the growth of s.c. A431, GBM-18, BxPC-3, and SK-RC-29 tumors compared to control groups ($P < 0.001$ for all tumor models). In the A431, BxPC-3, and SK-RC-29 models, tumor growth was completely inhibited, whereas in the GBM-18 model, tumor regression was observed in some animals. Results of human tumor xenograft studies are summarized in Table 1. In all human tumor xenograft models, inhibition of tumor growth was observed with a delay of 5–8 days following the start of DC101 treatment. No relapse of tumor growth was observed with continued administration of DC101 for up to 120 days in the A431 xenograft model (data not shown). Withdrawal of DC101 treatment resulted in resumed growth of all tumors with kinetics similar to controls after a lag period of approximately 10–14 days (data not shown). Tumors derived from DC101-treated animals appeared pale or translucent with diminished vasculature and permeability (Fig. 5, *B* and *C*). In contrast, large tumors with extensive vascularization that were highly permeable were observed in control groups.

**Anti-Flk-1 mAb Treatment Results in Tumor Cell and Endothelial Cell Apoptosis, Tumor Necrosis, and Decreased Vessel Density.** Histological examination of human xenograft tumors taken at different time points during therapy demonstrated dramatic differ-

Table 1 *Summary of inhibition of tumor growth with anti-Flk-1 mAb DC101*
DC101 or control IgG was administered i.p. at 800 $\mu$g/dose every 3 days.

| Tumor | *n* | % inhibition (day) | *P* value |
|---|---|---|---|
| Lewis lung | 10 | 70 (34) | <0.02 |
| 4T1 | 10 | 73 (35) | <0.02 |
| B16 | 10 | 75 (27) | <0.05 |
| A431 | 10 | 87 (44) | 0.001 |
| BxPC-3 | 10 | 79 (63) | 0.001 |
| GBM-18 | 10 | 92 (64) | 0.001 |
| SKRC-29 | 10 | 75 (60) | 0.001 |

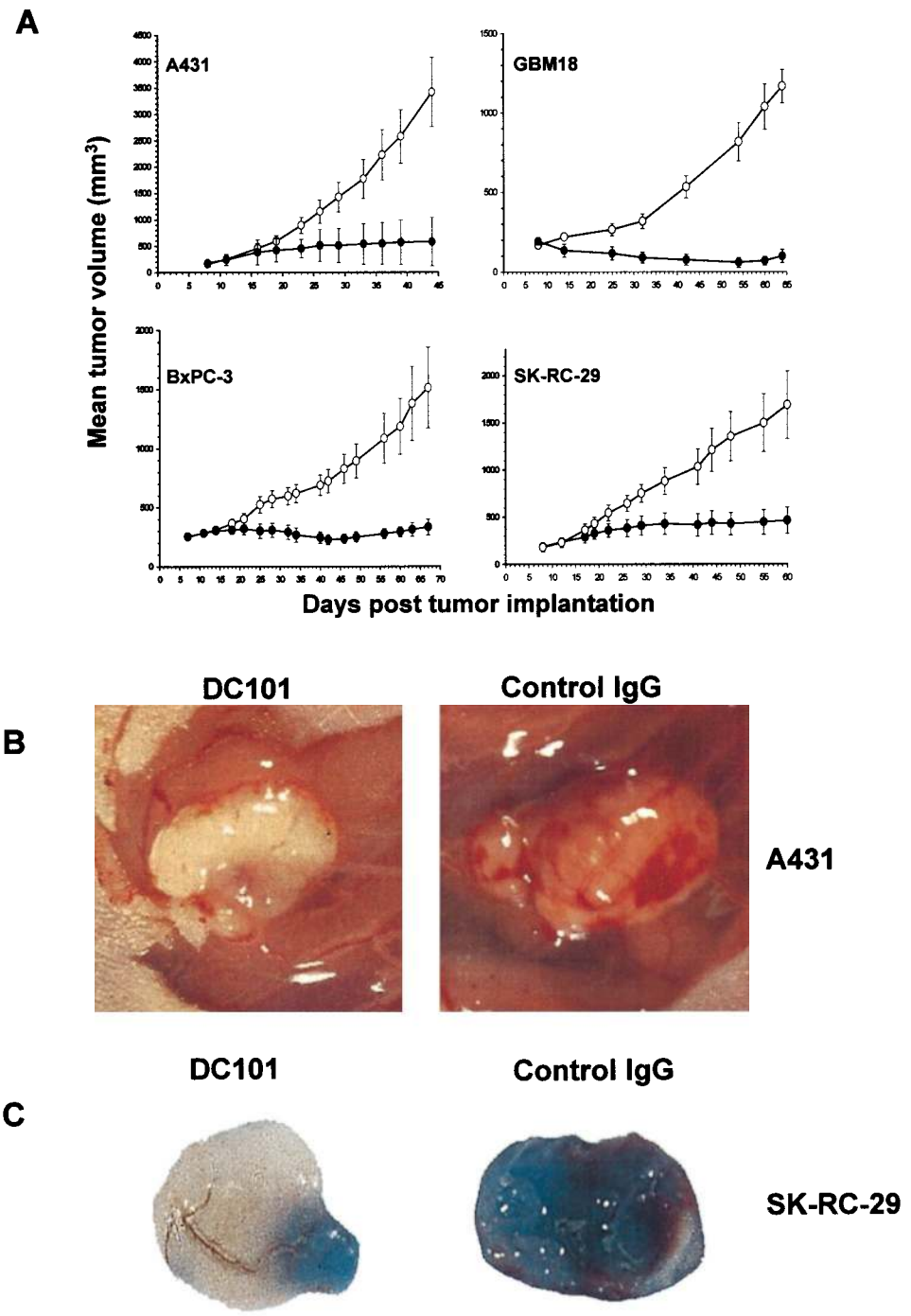


Fig. 5. Growth of s.c. human tumor xenografts in nude mice is inhibited by anti-Flk-1 mAb. Human epidermoid (A431), renal cell carcinoma (SK-RC-29), pancreatic (BxPC-3), or glioblastoma (GBM-18) tumors were established by injecting athymic nude mice s.c in the right flank with $2 \times 10^6$ tumor cells mixed in Matrigel. Tumors were allowed to reach 150–200 $mm^3$ in size and then randomized groups of mice received i.p. injections of either DC101 or control IgG (800 $\mu$g/dose) every 3 days. *A, data points,* mean tumor volumes of 10 mice/group; *bars,* SE. *B,* representative A431 tumors from mice treated for 28 days with DC101 or control IgG. Note pale, avascular tumor in DC101 treatment group. *C,* example of reduced permeability in SK-RC-29 xenografts treated for 14 days with DC101 compared to control IgG. Permeability of tumors was demonstrated by infusion of Evans blue as described in "Materials and Methods." Note pale, avascular tumor in DC101 treatment group that is largely devoid of Evans blue.

ences in tumors from DC101-treated *versus* control animals. Microvessel density was examined in DC101- and control-treated tumors by immunostaining with anti-PECAM mAb. A marked decrease in endothelial cells and vessel structures was observed after 1 and 2 weeks of treatment in DC101-treated tumors compared to controls (Fig. 6*A*). Quantitation of microvessels showed that density was reduced by DC101 treatment 88% ($P = 0.002$) and 90% ($P = 0.005$) after 1 and 2 weeks, respectively (Fig. 6*B*). Accurate quantitation of tumor vasculature was not possible beyond 2 weeks of treatment due to the extensive tumor necrosis in DC101-treated tumors. A marked decrease in cellularity and large areas of necrosis replaced by fibrous tissue was observed in DC101-treated tumors (Fig. 7, *A* and *D*). Tumor necrosis was observed after 1 week of therapy and progressed during the course of DC101 treatment. A marked decrease in tumor cell proliferation, as measured by anti-PCNA immunostaining, as well as an increase in tumor cell apoptosis, was seen in DC101-treated tumors (Fig. 7, *B* and *E*). This was accompanied by an increase in tumor cell apoptosis in DC101-treated tumors (Fig. 7, *C* and *F*).

## DISCUSSION

The results of our study demonstrate that blockade of the Flk-1 receptor by systemic administration of the mAb DC101 inhibits angiogenesis in two *in vivo* models and the growth of several mouse and human tumors. The rationale for using an anti-Flk-1 mAb antagonist is that this approach allows for a highly specific and potent

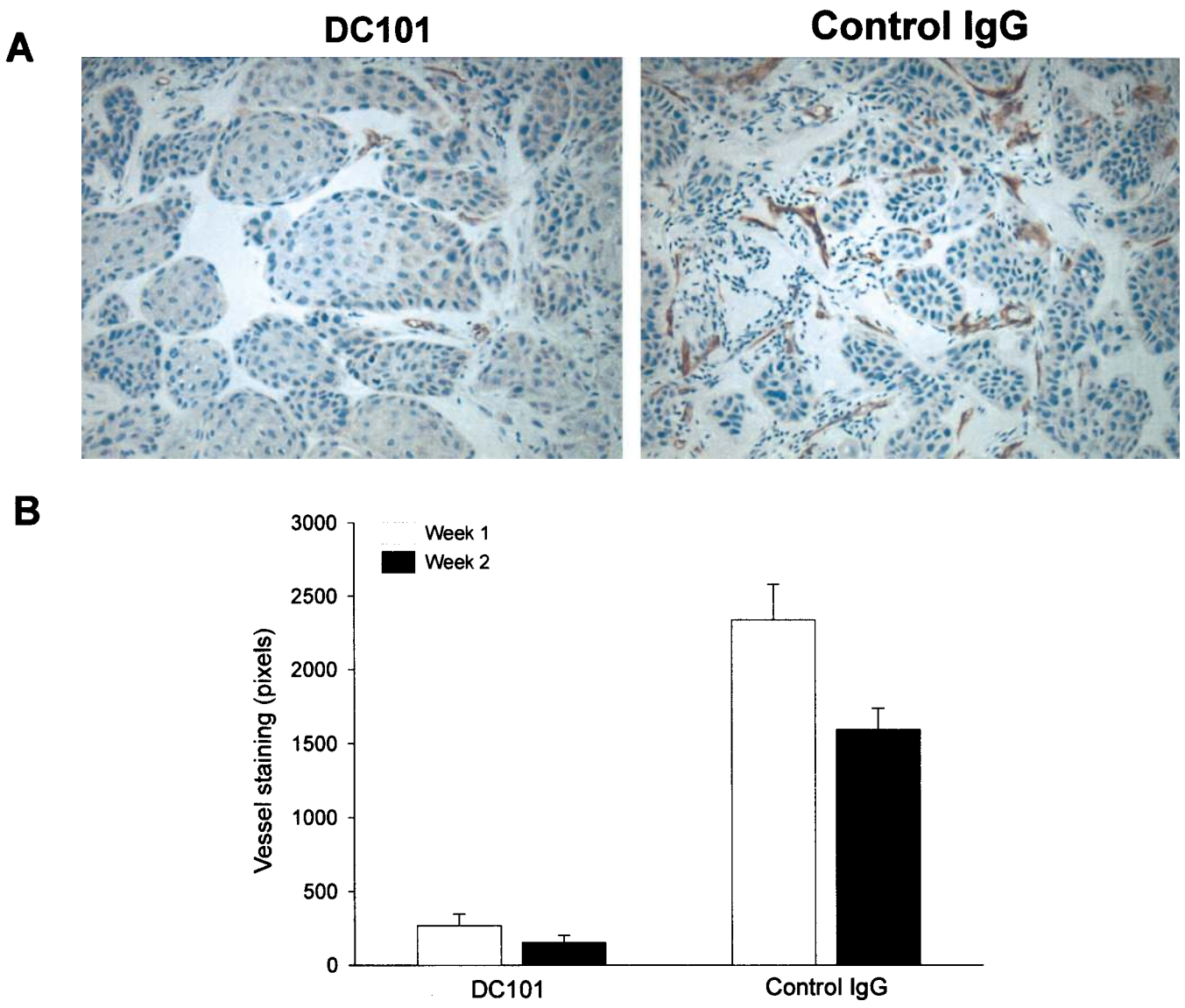


Fig. 6. Anti-Flk-1 mAb treatment reduces vessel density in tumors. *A,* A431 tumors from mice treated with control IgG or DC101 were resected after 1 week of antibody treatment, fixed, paraffin-embedded and sectioned at 7 um. Vessels were stained with biotinylated anti-PECAM antibody and visualized using streptavidin-HRP and DAB substrate. Endothelial cells and vessels (*brown*) were significantly reduced in DC101-treated tumors. ×200. *B,* A431 tumors from mice treated with control IgG or DC101 were resected after 1 (□) and 2 (■) weeks of antibody treatment and stained with anti-PECAM as described above. Microvessel density was quantitated by image analysis of stained sections as described in "Materials and Methods." A significant reduction ($P < 0.01$ *versus* control) in microvessel density was observed in the DC101 group after 1 and 2 weeks of treatment. *Columns,* mean; *bars,* SE.

means to block VEGF receptor function. Anti-Flk-1 mAb effectively inhibited neovascularization stimulated by growth factors (bFGF and VEGF) added to Matrigel plugs and neovascularization stimulated by tumor cells encapsulated in alginate beads. Previous studies in our laboratory have demonstrated that addition of both bFGF and VEGF to Matrigel significantly enhanced plug neovascularization compared to either factor alone.[3] Interestingly, in the present study we found that anti-Flk-1 mAb inhibited neovascularization of Matrigel plugs containing bFGF and VEGF. These data suggest that bFGF may induce or modulate a VEGF-dependent stage of angiogenesis, possibly by regulating expression of the Flk-1 receptor. In support of this hypothesis, we have found that bFGF up-regulates expression of VEGF and VEGF receptor (Flk-1/KDR) on endothelial cells.[4] Furthermore, we have found that anti-Flk-1 mAb also inhibits neovascularization of Matrigel plugs containing only bFGF.[3] Therefore, bFGF may up-regulate VEGF and/or VEGF receptor expression on endothelial cells *in vivo*, thus explaining inhibition of bFGF-induced neovascularization of Matrigel plugs by a VEGF receptor-specific mAb. A similar mechanism of inhibition most likely occurs during the process of tumor cell-stimulated angiogenesis as well.

To examine tumor growth in response to anti-Flk-1 mAb therapy, we chose the rapidly growing Lewis lung, 4T1, and B16 murine tumors. Treatment with DC101 markedly slowed the growth of Lewis lung, 4T1, or B16 primary tumors and significantly delayed the time period when these tumors reached a large size and mice became moribund. In addition, DC101 treatment inhibited the growth of disseminated Lewis lung metastases following removal of the primary tumor. These findings suggest that in addition to affecting the growth of a localized primary tumor, anti-Flk-1 mAb is also able to inhibit the dissemination and/or growth of distant metastases. It should be emphasized that anti-Flk-1 mAb therapy did not completely arrest primary tumor growth of these aggressive murine tumors. These tumors

[3] W. O'Connor, unpublished data.
[4] D. J. Hicklin, submitted for publication.

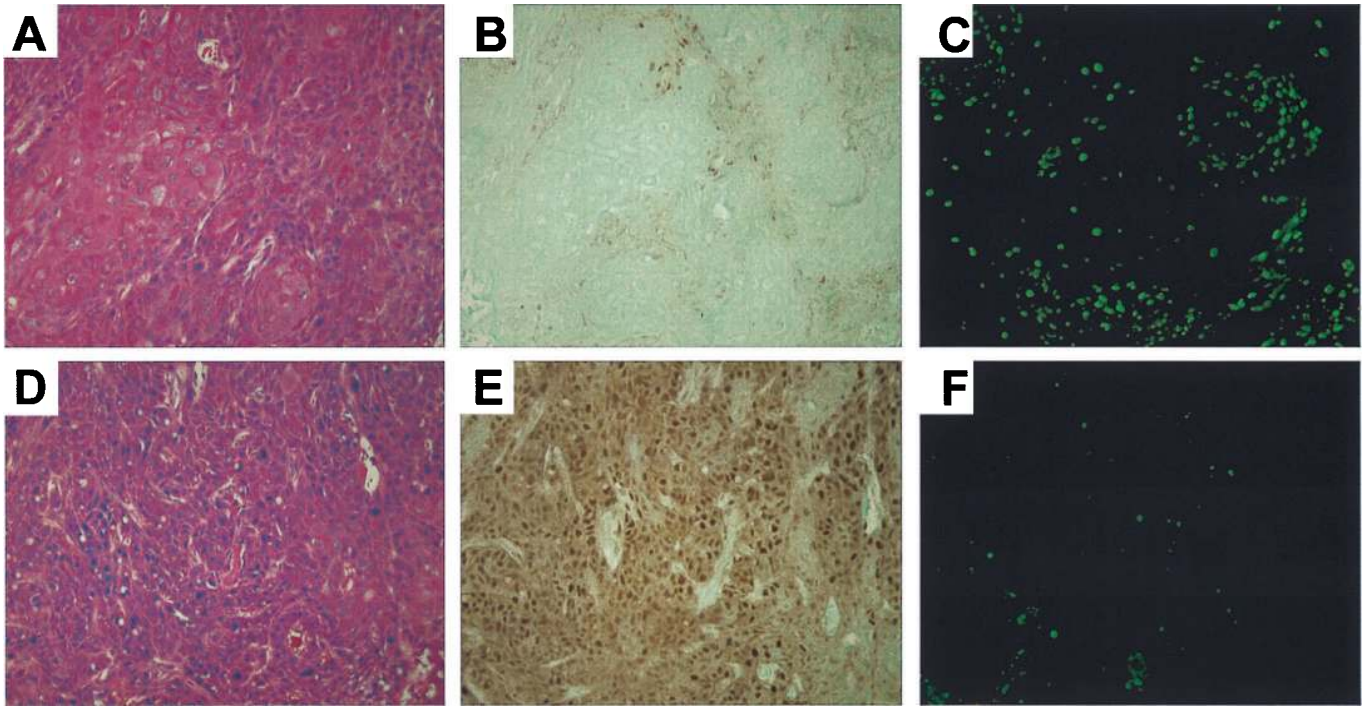


Fig. 7. Tumors treated with anti-Flk-1 mAb have increased tumor cell apoptosis, reduced tumor cell proliferation, and increased tumor necrosis. s.c. A431 tumors after 2 weeks of antibody therapy were resected, fixed, embedded in paraffin or frozen, and sectioned onto glass slides. Shown are representative sections from the DC101 group (*A–C*) and for the control IgG group (*D–F*). *A* and *D,* H&E staining of paraffin sections showed extensive areas of necrosis and fibrosis in tumors from DC101-treated animals. *B* and *E,* sections were immunostained with a mAb to PCNA (*brown*) and counterstained with eosin Y. The number of mitotic A431 tumor cells was significantly greater in tumors from control mice compared to tumors from DC101-treated animals. *C* and *F,* frozen sections of tumor tissue were assayed for apoptosis using a TUNEL kit that labels apoptotic nuclei with a fluorescent marker (*green*). A markedly higher frequency of apoptotic A431 tumor cells was found in tumors from DC101-treated animals. ×200.

may produce additional pro-angiogenic factors that allow their continued, albeit much reduced, growth in the presence of anti-Flk-1 blockade. DC101 did completely inhibit the growth of several human tumor xenografts in athymic mice. Typically, treatment of epidermoid, pancreatic, or renal tumors with DC101 resulted in cessation of tumor growth with only rare tumor regression. However, treatment of glioblastoma tumors with DC101 consistently resulted in tumor regressions, suggesting that this tumor is more susceptible to anti-Flk-1 therapy. It should be noted that no relapse of tumors was observed with continued administration of DC101 for up to 120 days (data not shown). Withdrawal of DC101 treatment in the various models tested resulted in regrowth of tumors with kinetics similar to that of control groups. The results of the present study are consistent with results obtained using a dominant-negative Flk-1 receptor (31), anti-VEGF mAb (33), VEGF antisense (32), or VEGF receptor tyrosine kinase inhibitors (39) and provide additional evidence for antiangiogenic and antitumor effects by blocking the VEGF/VEGF receptor pathway.

Histological examination of tumors from DC101-treated animals showed a decrease in microvessel density and an increase in apoptosis in the tumor cell fraction within the tumor. These findings coincided with a decrease in mitotic tumor cells within the tumor. The reduction in microvessels occurred rapidly, *i.e.,* after 1 week of treatment with DC101 and reached a peak after 14–21 days of treatment. The loss of microvessels within treated tumors suggests that VEGF stimulation of Flk-1-expressing tumor vasculature acts as a survival mechanism for proliferating tumor endothelium, which is inhibited by anti-Flk-1 therapy. This finding is consistent with previous studies that have shown VEGF prevents apoptotic death of microvascular endothelial cells (45, 46). Furthermore, Skobe *et al.* (47) have shown previously in a malignant keratinocyte invasion model that anti-Flk-1 mAb treatment inhibits endothelial cell proliferation and induces endothelial cell apoptosis that leads to vessel regression. These previous findings are consistent with the reduction in tumor vessel density in response to DC101 treatment found in the present study and suggest that similar mechanisms are involved. After 2 weeks of DC101 treatment, areas of necrosis developed in tumors that gradually increased as antibody treatment was continued. The mechanisms responsible for tumor cell apoptosis in DC101-treated tumors are not known. The decrease in tumor cell proliferation and necrosis in DC101-treated tumors likely reflects the lack of new vasculature that is needed to supply the rapidly growing tumor mass and may also indicate the lack of tumor cell survival factors provided by the tumor vasculature.

Angiogenesis inhibitors used as antitumor agents may need to be administered for longer periods than cytotoxic agents (48). It should be noted that we observed no toxicity associated with long-term treatment of tumor bearing animals. Autopsy of DC101-treated mice revealed no abnormalities in the organs of these mice, including the heart, intestine, kidney, liver, lung, and spleen. These findings are important, because low levels of Flk-1 expression are expected to be present on the endothelium of some normal tissues. The turnover of endothelial cells in normal adult tissues is very low (years) except in those tissues that undergo normal angiogenic processes, such as proliferation of the corpus luteum, pregnancy, and wound healing (13). Therefore, the lack of toxicity observed during anti-Flk-1 mAb therapy may be due to the limited dependence of resting endothelium for Flk-1/KDR stimulation. In contrast, tumor angiogenesis is expected to be more dependent on up-regulation and function of Flk-1/KDR on tumor vasculature and thus more susceptible to anti-Flk-1 blockade. The lack of toxicity associated with anti-Flk-1 mAb treatment can also be attributed to the high specificity of an antibody antagonist. It is conceivable that Flk-1/KDR blockade will have an impact on angiogenesis associated with reproduction, wound healing, or other normal processes involving angiogenesis, such as bone for-

mation. We are currently conducting studies to address these questions.

Combination therapy with anti-Flk-1 mAb and radiation or chemotherapeutic drugs may be a useful strategy because the use of these therapies alone are not able to completely eradicate tumors. In this regard, other antiangiogenic therapies have recently been used in combination with radiation (49) or chemotherapeutic drugs (50) showing an enhanced antitumor effect. Anti-Flk-1 therapy in combination with other antitumor agents may also provide an additive or synergistic effect. It could be argued that anti-Flk-1 treatment may actually reduce the efficacy of radiation or chemotherapeutics by reducing oxygenation of tumor tissue or permeability of tumors (51, 52). However, anti-Flk-1 therapy may increase drug delivery to a tumor, possibly by several mechanisms including lowering interstitial pressure, unpacking the mass of tumor cells, or transforming tumor vasculature to that of a "normal" vascular phenotype (51). Treatment with anti-Flk-1/KDR mAb also has the potential for increasing chemosensitivity or radiosensitivity of tumor vasculature. Because VEGF has been shown to act as a survival factor for endothelial cells in response to radiation or antineoplastic drugs (53, 54), anti-Flk-1/KDR therapy may block this protective effect on proliferating tumor vasculature. Studies are currently ongoing in our laboratory to address these questions.

In summary, we have demonstrated that anti-Flk-1 mAb DC101 effectively inhibits angiogenesis and tumor growth *in vivo*. These results suggest that blockade of the Flk-1/KDR receptor may be a useful strategy for treatment of human cancer. Furthermore, the use of anti-KDR therapy in combination with conventional cytotoxic, radiation, immunotherapy, or other antiangiogenic agents may improve the efficacy of these anticancer therapies. In this respect, Phase I trials are planned to evaluate anti-KDR therapy as a treatment for human cancer in a clinical setting.

## ACKNOWLEGMENTS

We thank Rajiv Bassi for excellent assistance in animal handling and N. Bander, L. Eisenbach, I. J. Fidler, P. Fisher, and K. Lyerly for supplying tumor cell lines.

## REFERENCES

1. Plate, K. H., Breier, G., and Risau, W. Molecular mechanisms of developmental and tumor angiogenesis. Brain Pathol., *4:* 207–218, 1994.
2. Hanahan, D., and Folkman, J. Patterns and emerging mechanisms of the angiogenic switch during tumorigenesis. Cell, *86:* 353–64, 1996.
3. Folkman, J., and Siegel, Y. Angiogenesis. J. Bio.. Chem., *267*. 10931–10934, 1992.
4. Nagy, J. A., Brown, L. F., Senger, D. R., Lanir, N., Van de Water, L., Dvorak, A. M., and Dvorak, H. F. Pathogenesis of tumor stroma generation: a critical role for leaky blood vessels and fibrin deposition. Biochim. Biophys. Acta. *948:* 305–326, 1989.
5. Klagsbrun, M., and D'Amore, P. A. Regulators of angiogenesis. Annun. Rev. Physiol., *53:* 217–239, 1991.
6. Dvorak, H. F., Nagy, J. A., Feng, D., Brown, L. F., and Dvorak, A. M. Vascular permeability factor/vascular endothelial growth factor and the significance of microvascular hyperpermeability in angiogenesis. Curr. Top. Microbiol. Immunol., *237:* 97–132, 1999.
7. Neufeld, G., Cohen, T., Gengrinovitch, S., and Poltorak, Z. Vascular endothelial growth factor (VEGF) and its receptors. FASEB J., *13:* 9–22, 1999.
8. Klagsbrun, M., and D'Amore, P. A. Vascular endothelial growth factor and its receptors. Cytokine Growth Factor Rev., *7:* 259–270, 1996.
9. Ferrara, N., Heinsohn, H., Walder, C. E., Bunting, S., and Thomas, G. R. The regulation of blood vessel growth by vascular endothelial growth factor. Ann. NY Acad. Sci., *752:* 246–256, 1995.
10. Senger, D. R., Perruzzi, C. A., Feder, J., and Dvorak, H. F. A highly conserved vascular permeability factor secreted by a variety of human and rodent tumor cell lines. Cancer Res., *46:* 5629–5632, 1986.
11. Leung, D. W., Cachianes, G., Kuang, W. J., Goeddel, D. V., and Ferrara, N. Vascular endothelial growth factor is a secreted angiogenic mitogen. Science (Washington DC), *246:* 1306–1309, 1989.
12. Plate, K. H., Breier, G., Weich, H. A., and Risau, W. Vascular endothelial growth factor is a potential tumor angiogenesis factor in human gliomas *in vivo*. Nature (Lond.), *359:* 8435–8438, 1992.
13. Peters, K. G., De Vries, C., and Williams, L. T. Vascular endothelial growth factor receptor expression during embryogenesis and tissue repair suggests a role in endothelial differentiation and blood vessel growth. Proc. Natl. Acad. Sci. USA, *90:* 8915–8919, 1993.
14. Fong, G. H., Rossant, J., Gertsenstein, M., and Breitman, M. L. Role of the Flt-1 receptor tyrosine kinase in regulating the assembly of vascular endothelium. Nature (Lond.), *376:* 66–70, 1995.
15. Matthews, W., Jordan, C. T., Gavin, M., Jenkins, N. A., Copeland, N. G., and Lemischka, I. R. A receptor tyrosine kinase cDNA isolated from a population of enriched primitive hematopoietic cells and exhibiting close genetic linkage to c-kit. Proc. Natl. Acad. Sci. USA, *88:* 9026–9030, 1991.
16. Terman, B. I., Dougher-Vermazen, M., Carrion, M. E., Dimitrov, D., Armellino, D. C., Gospodarowicz, D., and Bohlen, P. Identification of the KDR tyrosine kinase as a receptor for vascular endothelial cell growth factor. Biochem. Biophys. Res. Commun., *187:* 1579–1586, 1992.
17. Ferrara, N., Carver-Moore, K., Chen, H., Dowd, M., Lu, L., O'Shea, K. S., Powell-Braxton, L., Hillan, K. J., and Moore, M. W. Heterozygous embryonic lethality induced by targeted inactivation of the VEGF gene. Nature (Lond.), *380:* 439–442, 1996.
18. Shalaby, F., Rossant, J., Yamaguchi, T. P., Gersenstein, M., Wu, X.-F., Breitman, M. L., and Schuh, A. C. Failure of blood-island formation and vasculogenesis in Flk-1 deficient mice. Nature (Lond.), *376:* 62–66, 1995.
19. Dvorak, H. F., Soiussat, T. M., Brown, L. F., Berse, B., Nagy, J. A., Sotrel, A., Manseau, E. J., Van de Water, L., and Senger, D. R. Distribution of vascular permeability factor (vascular endothelial growth factor) in tumors: concentration in tumor blood vessels. J. Exp. Med., *174:* 1275–1278, 1991.
20. Shweiki, D., Itin, A., Soffer, D., and Keshet, E. Vascular endothelial growth factor induced by hypoxia may mediate hypoxia-initiated angiogenesis. Nature (Lond.), *359:* 843–845, 1992.
21. O'Brien, T., Cranston, D., Fuggle, S., Bicknell, R., and Harris, A. L. Different angiogenic pathways characterize superficial and invasive bladder cancer. Cancer Res., *55:* 510–513, 1995.
22. Brown, L. F., Berse, B., Jackman, R. W., Tognazzi, K., Guidi, A. J., Dvorak, H. F., Senger, D. R., Connolly, J. L., and Schnitt, S. J. Expression of vascular permeability factor (vascular endothelial growth factor) and its receptors in breast cancer. Hum. Pathol., *6:* 86–91, 1995.
23. Yoshiji, H., Gomez, D. E., Shibuya, M., and Thorgeirsson, U. P. Expression of vascular endothelial growth factor, its receptor, and other angiogenic factors in human breast cancer. Cancer Res., *56:* 2013–2016, 1996.
24. Takahashi, Y., Kitadai, Y., Bucana, C. D., Cleary, K. R., and Ellis, L. M. Expression of vascular endothelial growth factor and its receptor, KDR, correlates with vascularity, metastasis, and proliferation of human colon cancer. Cancer Res., *55:* 3964–8968, 1995.
25. Ellis, L. M., Staley, C. A., Liu, W., Fleming, R. Y., Parikh, N. U., Bucana, C. D., and Gallick, G. E. Down-regulation of vascular endothelial growth factor in a human colon carcinoma cell line transfected with an antisense expression vector specific for c-src. J. Biol. Chem., *273:* 1052–1057, 1998.
26. Brown, L. F., Berse, B., Jackman, R. W., Tognazzi, K., Manseau, E. J., Senger, D. R., and Dvorak, H. F. Expression of vascular permeability factor (vascular endothelial growth factor) and its receptors in adenocarcinomas of the gastrointestinal tract. Cancer Res., *53:* 4727–4735, 1993.
27. Plate, K. H., Breier, G., Weich, H. A., Mennel, H. D., and Risau, W. Vascular endothelial growth factor and glioma angiogenesis: coordinate induction of VEGF receptors, distribution of VEGF protein and possible *in vivo* regulatory mechanisms. Int. J. Cancer, *59:* 520–529, 1994.
28. Takahashi, A., Sasaki, H., Jin Kim, S., Kakizoe, T., Miyao, N., Sugimura, T., Terada, M., and Tsukamoto, T. Identification of receptor genes in renal cell carcinoma associated with angiogenesis by differential hybridization technique. Biochem. Biophys. Res. Commun., *257:* 855–859, 1999.
29. Stitt, A. W., Simpson, D. A., Boocock, C., Gardiner, T. A., Murphy, G. M., and Archer, D. B. Expression of vascular endothelial growth factor (VEGF) and its receptors is regulated in eyes with intra-ocular tumours. J. Pathol., *186:* 306–312, 1998.
30. Rossler, J., Breit, S., Havers, W., and Schweigerer, L. Vascular endothelial growth factor expression in human neuroblastoma: up-regulation by hypoxia. Int. J. Cancer, *81:* 113–117, 1999.
31. Millauer, B., Shawver, L. K., Plate, K. H., Risau, W., and Ullrich, A. Glioblastoma growth inhibited *in vivo* by a dominant-negative Flk-1 mutant. Nature (Lond.), *367:* 576–579, 1994.
32. Im, S. A., Gomez-Manzano, C., Fueyo, J., Liu, T. J., Ke, L. D., Kim, J. S., Lee, H. Y., Steck, P. A., Kyritsis, A. P., and Yung, W. K. Anti-angiogenesis treatment for gliomas: transfer of antisense-vascular endothelial growth factor inhibits tumor growth *in vivo*. Cancer Res., *59:* 895–900, 1999.
33. Kim, K. J., Li, B., Winer, J., Armanini, M., Gillett, N., Phillips, H. S., and Ferrara, N. Inhibition of vascular endothelial growth factor-induced angiogenesis suppresses tumour growth *in vivo*. Nature (Lond.) *362:* 841–844, 1993.
34. Kendell, R. L., and Thomas, K. A. Inhibition of vascular endothelial growth factor activity by endogenously encoded soluble receptor. Proc. Natl. Acad. Sci. USA, *90:* 10705–10709, 1993.
35. Lin, P. Sankar, S., Shan, S., Dewhirst, M. W., Polverini, P. J., Quinn, T. Q., and Peters, K. G. Inhibition of tumor growth by targeting tumor endothelium using a soluble vascular endothelial growth factor receptor. Cell Growth Differ., *9:* 49–58, 1998.
36. Fong, T. A., Shawver, L. K., Sun, L., Tang, C., App, H., Powell, T. J., Kim, Y. H., Schreck, R., Wang, X., Risau, W., Ullrich, A., Hirth, K. P., and McMahon, G. SU5416 is a potent and selective inhibitor of the vascular endothelial growth factor

receptor (Flk-1/KDR) that inhibits tyrosine kinase catalysis, tumor vascularization, and growth of multiple tumor types. Cancer Res., *59:* 99–106, 1999.
37. Rockwell, P., Neufeld, G., Glassman, A., Caron, D., and Goldstein, N. I. *In vitro* neutralization of vascular endothelial growth factor activation of Flk-1 by a monoclonal antibody. Mol. Cell. Differ., *3:* 91–109, 1995.
38. Zhu, Z., Rockwell, P., Lu, D., Kotanides, H., Pytowski, B., Hicklin, D. J., Bohlen, P., and Witte, L. Inhibition of vascular endothelial growth factor-induced receptor activation with anti-kinase insert domain-containing receptor single-chain antibodies from a phage display library. Cancer Res., *58:* 3209–3214, 1998.
39. Witte, L., Hicklin, D. J., Zhu, Z., Pytowski, B., Kotanides, H., Rockwell, P., and Bohlen, P. Monoclonal antibodies targeting the VEGF receptor-2 (Flk1/KDR) as an anti-angiogenic therapeutic strategy. Cancer Metastasis Rev., *17:* 155–161, 1998.
40. Tessler, S., Rockwell, P., Hicklin, D., Cohen, T., Levi, B. Z., Witte, L., Lemischka, I. R., and Neufeld, G. Heparin modulates the interaction of VEGF165 with soluble and cell associated Flk-1 receptors. J. Biol. Chem *269:* 12456–12461. 1994.
41. Passaniti, A., Taylor, R. M., Pili, R., Guo, Y., Long, P. V., Haney, J. A., Pauly, R. R., Grant, D. S., and Martin, G. R. A simple, quantitative method for assessing angiogenesis and antiangiogenic agents using reconstituted basement membrane, heparin, and fibroblast growth factor. Lab. Invest., *67:* 519–528, 1992.
42. Hoffmann, J., Schirner, M., Menrad, A., and Schneider, M. R. A highly sensitive model for quantification of *in vivo* tumor angiogenesis induced by alginate-encapsulated tumor cells. Cancer Res., *57:* 3847–3851, 1997.
43. Eisenbach, L., Hollander, N., Greenfeld, L., Yakor, H., Segal, S., and Feldman, M. The differential expression of H-2K *versus* H-2D antigens, distinguishing high-metastatic from low-metastatic clones, is correlated with the immunogenic properties of the tumor cells. Int. J. Cancer, *34:* 567–573, 1984.
44. Uyama, O., Okamura, N., Yanase, M., Narita, M., Kawabata, K., and Sugita, M. Quantitative evaluation of vascular permeability in the gerbil brain after transient ischemia using Evans blue fluorescence. J. Cereb. Blood Flow Metab., *8:* 282–284, 1988.
45. Alon, T., Hemo, I., Itin, A., Pe'er, J., Stone, J., and Keshet, E. Vascular endothelial growth factor acts as a survival factor for newly formed retinal vessels and has implications for retinopathy of prematurity. Nat. Med., *1:* 1024–1028, 1995.
46. Watanabe, Y., and Dvorak, H. F. Vascular permeability factor/vascular endothelial growth factor inhibits anchorage-disruption-induced apoptosis in microvessel endothelial cells by inducing scaffold formation. Exp. Cell Res., *233:* 340–349, 1997.
47. Skobe, M., Rockwell, P., Goldstein, N., Vosseler, S., and Fusenig, N. Halting angiogenesis suppresses carcinoma cell invasion. Nature Med., *11:* 1222–1227, 1997.
48. Folkman, J. Seminars in Medicine of the Beth Israel Hospital, Boston. Clinical applications of research on angiogenesis. N. Engl. J. Med., *333:* 1757–1763, 1995.
49. Mauceri, H. J., Hanna, N. N., Beckett, M. A., Gorski, D. H., Staba, M. J., Stellato, K. A., Bigelow, K., Heimann, R., Gately, S., Dhanabal, M., Soff, G. A., Sukhatme, V. P., Kufe, D. W., and Weichselbaum, R. R. Combined effects of angiostatin and ionizing radiation in antitumour therapy. Nature (Lond.), *394:* 287–291, 1998.
50. Teicher, B. A., Williams, J. I., Takeuchi, H., Ara, G., Herbst, R. S., and Buxton, D. Potential of the aminosterol, squalamine in combination therapy in the rat 13,762 mammary carcinoma and the murine Lewis lung carcinoma. Anticancer Res., *18:* 2567–2573, 1998.
51. Teicher, B. A. Hypoxia and drug resistance. Cancer Metastasis Rev., *13:* 139–168, 1994.
52. Rockwell, S. Oxygen delivery: implications for the biology and therapy of solid tumors. Oncol. Res., *9:* 383–390, 1997.
53. Katoh, O., Tauchi, H., Kawaishi, K., Kimura, A., and Satow, Y. Expression of the vascular endothelial growth factor (VEGF) receptor gene, KDR, in hematopoietic cells and inhibitory effect of VEGF on apoptotic cell death caused by ionizing radiation. Cancer Res., *55:* 5687–5692, 1995.
54. Katoh, O., Takahashi, T., Oguri, T., Kuramoto, K., Mihara, K., Kobayashi, M., Hirata, S., and Watanabe, H. Vascular endothelial growth factor inhibits apoptotic death in hematopoietic cells after exposure to chemotherapeutic drugs by inducing MCL1 acting as an antiapoptotic factor. Cancer Res., *58:* 5565–5569, 1998.